NRC·CNRC

NRC Publications Archive
Archives des publications du CNRC

Monitoring Lentiviral Vector Production Kinetics Using Online Permittivity Measurements

Ansorge, Sven; Lanthier, Stqphane; Transfiguracion, Julia; Henry, Olivier; Kamen, Amine

This publication could be one of several versions: author's original, accepted manuscript or the publisher's version. / La version de cette publication peut être l'une des suivantes : la version prépublication de l'auteur, la version acceptée du manuscrit ou la version de l'éditeur.
For the publisher's version, please access the DOI link below./ Pour consulter la version de l'éditeur, utilisez le lien DOI ci-dessous.

Publisher's version / Version de l'éditeur:
https://doi.org/10.1016/j.bej.2011.01.002
Biochemical Engineering Journal, 54, 1, pp. 16-25, 2011-01-07

NRC Publications Record / Notice d'Archives des publications de CNRC:
https://nrc-publications.canada.ca/eng/view/object/?id=70c5e382-ff79-48cb-b6e7-e3c2668d742d
https://publications-cnrc.canada.ca/fra/voir/objet/?id=70c5e382-ff79-48cb-b6e7-e3c2668d742d

Access and use of this website and the material on it are subject to the Terms and Conditions set forth at
https://nrc-publications.canada.ca/eng/copyright
READ THESE TERMS AND CONDITIONS CAREFULLY BEFORE USING THIS WEBSITE.

L'accès à ce site Web et l'utilisation de son contenu sont assujettis aux conditions présentées dans le site
https://publications-cnrc.canada.ca/fra/droits
LISEZ CES CONDITIONS ATTENTIVEMENT AVANT D'UTILISER CE SITE WEB.

Questions? Contact the NRC Publications Archive team at PublicationsArchive-ArchivesPublications@nrc-cnrc.gc.ca. If you wish to email the authors directly, please see the first page of the publication for their contact information.

Vous avez des questions? Nous pouvons vous aider. Pour communiquer directement avec un auteur, consultez la première page de la revue dans laquelle son article a été publié afin de trouver ses coordonnées. Si vous n'arrivez pas à les repérer, communiquez avec nous à PublicationsArchive-ArchivesPublications@nrc-cnrc.gc.ca.

National Research Council Canada | Conseil national de recherches Canada

Canada

Biochemical Engineering Journal xxx (2011) xxx–xxx

Contents lists available at ScienceDirect

Biochemical Engineering Journal

journal homepage: www.elsevier.com/locate/bej

Monitoring lentiviral vector production kinetics using online permittivity measurements

Sven Ansorge[a,b], Stéphane Lanthier[a], Julia Transfiguracion[a], Olivier Henry[b], Amine Kamen[a,b,*]

[a] National Research Council Canada, Biotechnology Research Institute, 6100 Royalmount Avenue, Montréal, Québec H4P 2R2, Canada
[b] École Polytechnique de Montréal, C.P. 6079, succ. Centre-ville, Montréal, Québec H3C 3A7, Canada

ARTICLE INFO

Article history:
Received 19 August 2010
Received in revised form
20 December 2010
Accepted 7 January 2011
Available online xxx

Keywords:
Lentiviral vector production
HEK293
Perfusion culture
Online monitoring
Permittivity measurements
Dielectric spectroscopy
Process Analytical Technology (PAT)

ABSTRACT

Lentiviral vectors (LVs) are effective delivery vehicles that have been successfully used in gene and cell therapy. LVs are most commonly produced via the transient transfection of several plasmid constructs in adherent cell cultures. Recently, we described an efficient and scalable LV production in serum-free suspension cultures. To further facilitate the translation of LV-based interventions to the clinic, the robustness of the production process needs to be ensured to ultimately achieve a specified quality and quantity of LV production lots. However, routine processes are largely empirical, and strategies to monitor LV production kinetics in real-time have not yet been described.

In this work, *in situ* real-time permittivity measurements were assessed to document the production of LVs. Characteristic process phases that were closely associated with LV production kinetics were identified. The permittivity signal evolution was interpreted by exploiting various independent online and offline monitoring measurements. Cellular membrane properties and, to a lesser extent, cell size were the main factors contributing to the permittivity variations. It is concluded that the permittivity-related parameters can be used for the detection of viral release, allowing real-time assessment of process performance. The technology should thus greatly facilitate process development and optimization.

Crown Copyright © 2011 Published by Elsevier B.V. All rights reserved.

1. Introduction

The most advanced generations of lentiviral vectors (LVs) are safe and potent tools for gene and cell therapy interventions [1,2]. Most LVs are derived from human immunodeficiency virus type 1 (HIV-1), and they possess several advantages over other virus-based gene delivery vehicles, such as a large packaging capacity, the ability to infect non-dividing cells and the absence of transferred viral coding sequences [1,3].

However, despite recent progress in the field, the mass production of LVs remains an important limitation for the translation of LV-based therapeutic strategies to the clinic [4,5]. Current processes are generally not sufficiently robust to support the industrial manufacturing of these promising vectors. For LVs as well as other vectors, such as adeno-associated viruses (AAV), transfection currently remains the most effective option for mass production due to the difficulty and time required to generate stable producer cell lines [6,7].

Large-scale transient transfection has already been used for the production of proteins and viral vectors to generate preclinical and clinical material in a timely manner [8–11]. However, these early generation processes are generally not well characterized due to the lack of detailed key process parameter monitoring and sub-optimal control of bioreactor culture conditions. Therefore, one avenue for the optimization of transfection processes is the identification, characterization and control of critical process parameters to ensure robustness and reduce batch to batch variability [12]. Consequently, to establish industrially viable LV production processes, reliable monitoring tools that either directly quantify the vectors and/or reflect their release from the producer cells are required. The implementation of these techniques is generally a prerequisite to efficiently characterize cell culture operations, which in turn facilitates their development and optimization and ensures process consistency and robustness during production [13].

From another stand point, although there has been a constant interest in monitoring and control technologies since the beginning of the industrial cell culture era, a renewed interest has been generated from the release of FDA's guidance on Process Analytical Technology (PAT). The PAT initiative proposes a shift of biomanufacturing quality control from the laboratory to the process site, enabling a "Quality by Design" that results in

* Corresponding author at: National Research Council Canada, Biotechnology Research Institute, 6100 Royalmount Avenue, Montréal, Québec H4P 2R2, Canada.
E-mail address: amine.kamen@cnrc-nrc.gc.ca (A. Kamen).

1369-703X/$ – see front matter. Crown Copyright © 2011 Published by Elsevier B.V. All rights reserved.
doi:10.1016/j.bej.2011.01.002

Please cite this article in press as: S. Ansorge, et al., Monitoring lentiviral vector production kinetics using online permittivity measurements, Biochem. Eng. J. (2011), doi:10.1016/j.bej.2011.01.002

a pre-defined, i.e., a 'built-in' final product quality. A successful application of a PAT-based strategy requires technologies and tools operating *in situ*, being non-invasive and generating online information about multiple key bioprocess and/or metabolic variables [14]. These monitoring tools should provide global, macroscopic bioprocess outputs, ensuring their versatile and flexible utilization in different production systems.

The biomass content is the most important variable to monitor and control in any cell culture process [15–17]. Online *in situ* probes based on dielectric spectroscopy (permittivity measurements) are established tools for biomass monitoring. Unlike most other online approaches based upon the correlation of metabolic rates with cell density (e.g., oxygen uptake rate (OUR) measurements), permittivity measurements provide more direct information on the biomass content. They are easily transferable to different bioreactor scales and, as such, hold great promise for applications in process development. Moreover, permittivity measurements have the potential to provide additional meaningful real-time information for process control and optimization. Their use to monitor critical transition points in cell culture processes was previously described during the production of baculovirus expression vectors (BEV) [18,19] and has recently been further studied in mammalian cell culture systems [20,21]. These transition points are typically related to significant changes in cellular dielectric properties, occurring when cell physiology, morphology or metabolism is altered.

Upon viral infection, the initial release and the production of progeny virus are generally associated with significant physiological changes in the host cells. These physiological changes, when taking place in the plasma membrane in particular, directly affect the dielectric properties of the cells. Several studies describe the monitoring of the effects caused by viral infection using techniques such as electrorotation on single cells [22,23]. Yet, to date, the application of these findings, i.e., the use of permittivity measurements in virus or viral vector production, is limited to BEV production. After infection of insect cell cultures with the baculovirus, BEV replication results in changes of the host cell physiology and morphology, most notably a dramatic increase in the mean cell diameter. This change in cell size can be monitored in real-time and used to predict the success and efficiency of the infection [24,25]. The onset of the BEV budding from the cell membrane and its release in the supernatant is also reflected in the permittivity, in particular, when the infection is synchronous [18,19]. These findings were also helpful in the analysis of more complex systems in which BEVs are used to produce AAVs [26,27], allowing real-time determination of the optimum harvest point.

The goal of this study is to determine whether permittivity measurements could provide meaningful real-time information related to lentiviral vector release and production kinetics. LVs were produced by the transient transfection of suspension-grown HEK293 producer cells using a perfusion process in which functional LV particles are rapidly harvested to address their low stability at 37 °C. The online permittivity data were correlated with changes in biovolume and cell diameter and were compared with viral production kinetics, changes in oxygen consumption and GFP expression. Significant changes in the permittivity-related real-time signals indicated the first viral release and the progress of LV production. Characteristic process phases were identified based on the online data, which were observed during LV production using different operating conditions. In addition, the online permittivity signal variations can be correlated with the total viral particle yield. As this monitoring tool allows for the determination of vector release in real-time, it is concluded that permittivity measurements could be used to optimize the harvest time window and to provide early assessments of the process performances.

2. Materials and methods

2.1. Cell culture

HEK293SF-3F6 cells [28] were suspension-grown in HyQSFM4TransFx293 (HyQ) (Hyclone, Logan, UT), which was supplemented with Cell Boost 5 (CB5) at 5% (v/v) (Hyclone, Logan, UT) when indicated (HyQ+). Subcultures were passaged every 2–3 days to keep the cells in their exponential growth phase. Hemacytometer counts using erythrosine B dye exclusion were used to assess the cellular density (viable, total cell count per mL (*vcc*, *tcc*)) and viability.

2.2. Bioreactor LV production

2.2.1. Transient transfection

The transfection protocol and process development for high-yield LV production have been previously described in detail [29]. In brief, a GFP-encoding self-inactivating transfer vector (pCSII-CMV5-GFPq), third generation packaging plasmids (pMDLg/pRRE#54 and pRSV-Rev) and a vector encoding the VSV-G envelope (pSVCMV-IN-VSVg) [30,31] were simultaneously transfected into HEK293 cells to produce LVs. A plasmid mass ratio of 1:1:1:2 (VSV-G:Gag-Pol:Rev:Lentiviral Transfer Vector) [32] was used for the polyethylenimine (PEI)-mediated transfection, and sodium butyrate was added at a concentration of 5 mM, 16 h post-transfection, according to the previous results from our group [29].

2.2.2. Bioreactor cultures

The bioreactor setup was identical to the one used in a previous study [29]; similar conditions have been described earlier in detail [33]. In brief, a Chemap 3.5 L type SG bioreactor vessel (working volume 2.7 L) was equipped with probes to measure and control the temperature and dissolved oxygen (DO) at 37 °C and 40% air saturation. Agitation rate was set to 85 rpm and the pH was controlled in the range of 7.1–7.2 by the addition of CO_2 via the surface or sodium bicarbonate solution (7.5% (w/v)). In perfusion mode, cells were retained in the bioreactor using a 10 L acoustic filter (AppliSens, Schiedam, Netherlands) operated in backflush mode (full recycling of cell suspension into bioreactor at each backflush) with an interval of 30 min and a run/stop ratio of 55/5 s.

Cultures were grown in batch mode up to ~1 to 2×10^6 *vcc* when perfusion was started at 1 or 2 volume(s) of medium per reactor volume per day (VVD). After reaching the targeted cell density ($5–8 \times 10^6$ *vcc*) in perfusion mode, the culture was transfected by the addition of polyplexes. After transfection, the LV-containing supernatant was kept at 4 °C until clarification (once daily) and subsequently stored at −80 °C.

For the first 2 days of culture, surface aeration was used for the oxygen supply. After that, pure oxygen was pulse sparged into the culture at increasing flow rates (depending on the biomass content in the reactor) to control the DO. The total volume of oxygen (in mL) that was sparged into the culture was monitored. From this value, the derivative as the oxygen sparging rate (OSR in mL/min) was then calculated over time. This value was used as an indicator of the volumetric oxygen consumption. The overall aeration strategy was similar to what has been described earlier by our group [34].

2.3. Lentiviral quantification

2.3.1. Gene transfer assay

Functional viral titer (GTA titer) was determined using a flow cytometry-based gene transfer assay (GTA) [29,32]. In brief, HEK293E cells (clone 6E) were cultured in Freestyle™ 17 medium (Invitrogen) and diluted at the day of transduction to a cell density of 5.5×10^5 c/mL. Polybrene (SIGMA) was directly added to

Please cite this article in press as: S. Ansorge, et al., Monitoring lentiviral vector production kinetics using online permittivity measurements, Biochem. Eng. J. (2011), doi:10.1016/j.bej.2011.01.002

the cell suspension at 8 μg/mL. After 15–30 min of incubation at 37 °C, 0.9 mL of the cell suspension was loaded into each well of a 12 well plate and 0.1 mL of the diluted LV-containing samples were added. Two days later, the cells were harvested by centrifugation, resuspended in PBS and fixed by formaldehyde addition (final concentration of 2%). The samples were then scored for GFP expression by FACS analysis. The limit of detection of this assay is $\sim 1 \times 10^5$ tu/mL. An in-house LV standard was used in all GTA experiments to minimize inter-assay variability. All final titers were calculated relative to this LV standard, which was found to be stable over a period of more than 1 year after storage at −80 °C in culture medium. Transduction of the selected samples was performed in the presence of AZT (SIGMA) to rule out pseudotransduction.

2.3.2. Total viral particle quantification (VG titer) by real-time polymerase chain reaction (RT-PCR)

The VG titer, i.e., the amount of total viral particles expressed as viral genomes (vg/ml), was determined using a SYBR-Green® I (SGI) quantitative RNA PCR assay (Roche Applied Science, Laval, Qc). An in-house RNA standard was used to quantify LV in the supernatants from the production runs. After RNA purification from LV-containing supernatants using the High Pure Viral RNA kit (Roche Applied Science, Laval, Qc), samples were treated with DNAse (DNA-free Kit, Applied Biosystems, Foster City, CA). RT-PCR was then performed in a Carousel-based LightCycler (Roche Applied Science, Laval, Qc) or a Mastercycler ep realplex system (Eppendorff, Hamburg, Germany). Primers (P1, P2) targeting a sequence in the woodchuck hepatitis virus posttranscriptional regulatory element (WPRE) were selected using clone manager (Sci-Ed Software, Cary, NC). Each reaction had a volume of 20 μL with 0.5 μM of each primer (P1: LVWPREF: AGT-TGT-GGC-CCG-TTG-TCA-GG, P2: LVWPRER: AGG-CGA-GCA-GCC-ATG-GAA-AG), amplifying a sequence in the WPRE element of 249 bp. The RNA standard was produced using the MEGASCRIPT kit (Applied Biosystems, Foster City, CA). For this purpose, WPRE from the LV transfer vector (CSII-CMV-GFPq) was cloned into pUC19 T7. The resulting plasmid pUC19 T7-LVWPRE was then linearized and transcribed *in vitro*. The transcript (RNA standard), with a length of 260 bases, was purified (MEGACLEAR kit, Applied Biosystems, Foster City, CA), quantified by spectrophotometry and aliquoted at the final standard concentrations (1×10^9–1×10^4 copies/reaction) in DEPC-treated water. Specificity of the PCR reactions was confirmed by melting curve and agarose gel analyses. The lower detection limit of this method is in the range of 5×10^5 vg/mL.

2.4. Cell culture sample analyses

2.4.1. Cell size measurement

The volume-weighted arithmetic mean cell diameter (d) was determined using a Z2™ Coulter Counter® (Beckman Coulter, Mississauga, ON) with an aperture diameter of 100 μm, followed by analysis of the size distributions with the Accucomp® software package (Beckman Coulter). To dissociate the cellular aggregates which could affect the measurement, samples were subjected to scratching as described by Côté et al. [28], and, if necessary, diluted 1:2 in Accumax solution (eBioscience, San Diego, CA) and incubated for 15 min at 37 °C prior to analysis.

The lower and upper limits for the analysis were 7.31 and 23.8 μm, respectively. To calculate d, the distributions were plotted as volume (%) against cell diameter (μm). After acquisition of the cell size distribution, the lower limit was set to select the viable cell population in the cell size distribution. This was done to exclude cell debris and dead cells for which a smaller cell size is measured [35,36]. The resulting viable cell size distributions were evenly scattered around the mean cell diameter with low levels of positive skewness, representing 90–95% of the total measured volume for all samples.

Each value of d represents the average of at least two distributions assessed on the same sample. Using d and the viable cell count per mL (vcc), the biovolume (bv) was calculated using Eq. (1):

$$bv = \frac{4}{3} \times \left(\frac{d}{2}\right)^3 \times \pi \times vcc \quad (1)$$

In this study, the value of bv was an estimate of the volume fraction of cells P in the Schwan equation ([37,38,41]; see Section 2.5).

2.4.2. GFP measurement

The total expression of GFP was measured on a SpectraMax Gemini EM plate reader (Molecular Devices, Sunnyvale, CA) in 96-well plates. Approximately 1×10^5 cells were distributed into each well, and the fluorescence was measured at wavelengths of 485/538/495 nm (excitation/emission/cutoff) after fixation with 4% formaldehyde.

2.5. Permittivity measurements

In this study, a Biomass System® (Fogale nanotech, Nîmes, France) as well as a Biomass Monitor 220 (Aber Instruments, Aberystwyth, UK) were employed for the measurement of permittivity across the β-dispersion frequency spectrum of ∼0.1 to 10 MHz. Both systems provide the β-dispersion parameters ($\Delta\varepsilon_{max}$, fc, α) after fitting the frequency spectra. The calculation of the β-dispersion parameters was performed with commercially available software packages, either offline using AberScan (Aber Instruments) or in real-time with the Biomass 400 (Fogale nanotech). In addition, both systems measure the dual-frequency permittivity at different measurement frequencies in the β-dispersion range. The Biomass Monitor 220 (Aber Instruments, Aberystwyth, UK) measures $\Delta\varepsilon_{0.6\ MHz}$ at 0.6 and 19.5 MHz, whereas the Biomass System/Biomass 400 (Fogale nanotech, Nîmes, France) routinely operates at 1 and 10 MHz, providing $\Delta\varepsilon_{f_C}$.

The underlying theory on the dielectric properties of biological cells has been described in detail elsewhere, and readers should refer to this work for illustrations of and additional information on the β-dispersion [37–41]. In brief, when placed in an alternating electric field, any given cell suspension shows a characteristic decrease in permittivity with increasing frequency. This decrease, the β-dispersion, is caused by the polarization of cell membranes. The resulting dielectric/permittivity increment ($\Delta\varepsilon_{max}$) is directly correlated to the membrane-enclosed volume fraction, i.e., the biovolume (bv) of the cell suspension. For spherical cells at high viability (and therefore a low membrane conductivity) and for low biovolume levels as observed in mammalian cell culture, one can mathematically define this decrease by the following three parameters: permittivity increment ($\Delta\varepsilon_{max}$), characteristic frequency (f_C) and the Cole–Cole α (α) [Eq. (2)]. The first parameter $\Delta\varepsilon_{max}$ can be measured as the difference in permittivity at the low-frequency and the high-frequency plateau (permittivity increment) and is defined as:

$$\Delta\varepsilon_{max} = \frac{9 \times d/2 \times bv \times C_M}{4} \quad (2)$$

where $d/2$ is the cell radius (m), C_M is the capacitance per membrane area (F m^{-2}) and bv represents the biovolume [Eq. (1)]. Eq. (2) is essentially identical to the original equation of Schwan [37,38,41], except that for our analysis, the volume fraction of cells (P) was replaced by the biovolume (bv), as defined in Eq. (1).

The second parameter, the characteristic frequency (f_C), is the frequency at which the permittivity is decreased by half. The f_C can be defined by the following simplified equation [Eq. (3)]

Please cite this article in press as: S. Ansorge, et al., Monitoring lentiviral vector production kinetics using online permittivity measurements, Biochem. Eng. J. (2011), doi:10.1016/j.bej.2011.01.002

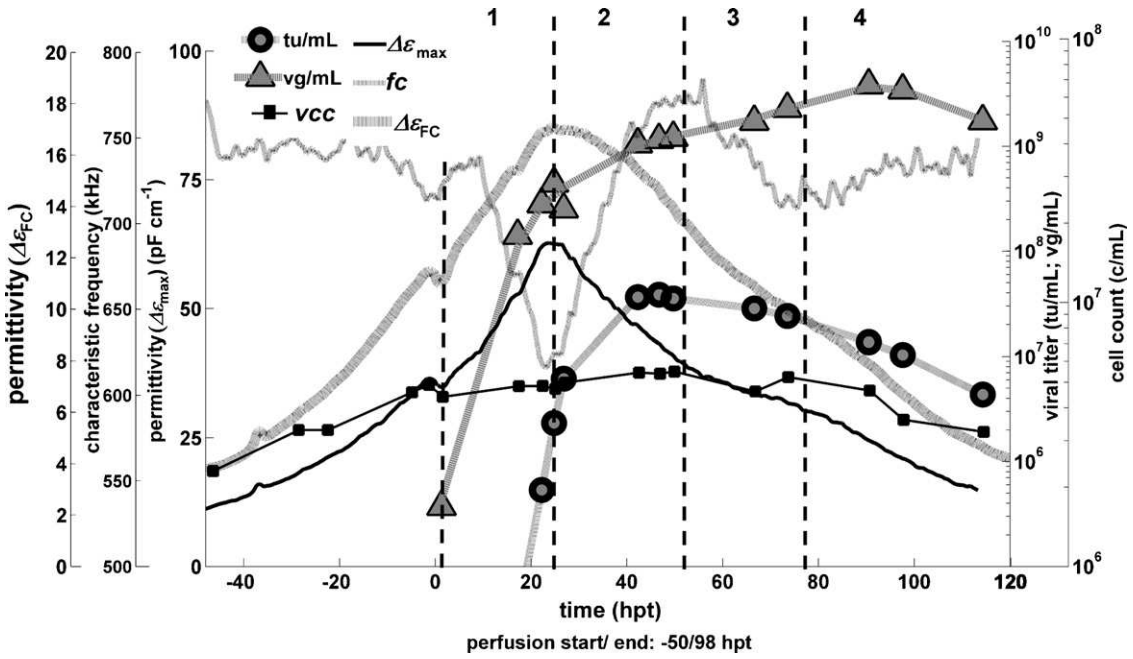

Fig. 1. High-yield LV production in bioreactor scale. After transfection, cell growth continued at a decreased rate until a maximum *vcc* of ~6×10^6 c/mL was reached ~48 h post-transfection (hpt). Dashed lines and numbers indicate characteristic process phases that were identified according to changes in permittivity and the related β-dispersion parameters.

[37,38,41,42]:

$$f_C = \frac{1}{2 \times \pi \times d/2 \times C_M \times (1/\sigma_i + 1/2\sigma_m)} \quad (3)$$

where σ_i is the conductivity of the cytoplasm (intracellular conductivity; mS cm^{-1}) and σ_m is the conductivity of the medium (mS cm^{-1}). Because the value of σ_m is generally much higher than σ_i in typical cell culture experiments, this equation can be further simplified by omitting the term $1/2\sigma_m$ [21].

A third parameter describing the β-dispersion is α (also known as: Cole–Cole α). It is an empirical parameter describing the decrease in permittivity with increasing frequency in the Cole–Cole equation [43]. The α parameter is generally associated with changes in the distribution of cellular electrical properties [44].

3. Results and discussion

3.1. LV production in bioreactor runs

3.1.1. Identification of characteristic process phases during LV production

In the preliminary batch and also the transfected cultures that resulted in a low yield, the permittivity profile followed the cell density increase very well and correlated with the biovolume that was measured offline throughout the entire culture period (data not shown). This is in line with results from others for batch cultivations of different cell lines [18,19,21].

The results of a representative experiment in which LVs were produced by transient transfection in bioreactor cultures are shown in Fig. 1. In this culture, cells were transfected at a *vcc* of ~5×10^6 c/mL. At the time of transfection, the small dilution of the cell suspension resulting from the addition of the polyplexes was reflected in the values of the permittivity ($\Delta\varepsilon_{fc}$) and its increment ($\Delta\varepsilon_{max}$). After transfection, *vcc* kept increasing at a significantly reduced rate, and the maximum *vcc* was observed at approximately 48 h post-transfection (hpt). In contrast, $\Delta\varepsilon_{max}$ and $\Delta\varepsilon_{fc}$ increased at a similar rate compared to the time before transfection and reached a maximum at approximately 24 hpt with $\Delta\varepsilon_{max}$ exhibiting a more distinct maximum compared to $\Delta\varepsilon_{fc}$. The characteristic frequency (*fc*) dropped significantly after the transfection, attaining a minimum at the time of the maximum in $\Delta\varepsilon_{fc}$ and $\Delta\varepsilon_{max}$. Functional LV particles (GTA titer as transducing units (tu)/mL), and total viral particles (VG titer as viral genomes (vg)/mL) were first measured in the supernatant at around 20 hpt, corresponding to the maximum in permittivity. A maximum GTA titer of approximately 4×10^7 tu/mL in the supernatant was found at around 48 hpt, after which an exponential decrease in GTA titer was observed. The VG titer showed a similar evolution from 20 to 40 hpt. However, after the maximum in functional viral particles was reached, the VG titer further increased until its maximum was attained at ~96 hpt. The overall LV production profile was thus broken down into four distinct process transition phases after transfection, defined according to the extrema and slope changes in the online permittivity signals $\Delta\varepsilon_{max}$ and *fc*. Phase 1 (0–24 hpt) was characterized by a relative increase in $\Delta\varepsilon_{max}$ of 80%, whereas the characteristic frequency (*fc*) decreased by 13% and reached a minimum at the time of the maximum in $\Delta\varepsilon_{max}$. During the second phase (24–50 hpt), $\Delta\varepsilon_{max}$ was found to decrease by ~38%, while *fc* increased by ~28%. This phase ended when *fc* reached its maximum, which coincided with a slope change in the permittivity increment. During phase 3 (50–75 hpt), the values of $\Delta\varepsilon_{max}$ and *fc* both decreased gradually. The onset of the last phase (75–120 hpt) corresponded to a second minimum in *fc*, paralleled by a slope change in $\Delta\varepsilon_{max}$.

Although LV release in the form of transducing particles were detected at low levels as early as at the end of phase 1, significant amounts of viral titers, i.e., 10–100% of the peak GTA titer, and up to 30% of the peak VG titer in the bioreactor supernatant were not detected before the beginning of phase 2. It was therefore hypothesized that the extrema in $\Delta\varepsilon_{max}$ and *fc* at the transition from phase 1 to phase 2 were related to this initial viral release after transfection. The subsequent changes also corresponded with events related to LV production, such as the transition into phase 3 at which the maximum functional viral titer in the reactor was attained. Finally, at the beginning of phase 4, functional LV titers had significantly decreased (<30%). In contrast, the VG titer remained stable, indicat-

Please cite this article in press as: S. Ansorge, et al., Monitoring lentiviral vector production kinetics using online permittivity measurements, Biochem. Eng. J. (2011), doi:10.1016/j.bej.2011.01.002

ing that a large number of non-functional viral particles containing viral RNA were constantly produced after the transfection.

The characteristic process phases that were identified based on *in situ* permittivity measurements showed significant differences in LV productivity and appeared to be thus linked to the functional viral titer in the reactor supernatant. Functional LVs present a low half-life of 3–18 h [45], and we observed values of ~13 h for LVs incubated in cell-free bioreactor supernatants at 37 °C compared to 40–50 h at 4 °C [unpublished results]. As we described earlier [29], production in perfusion cultures is thus advantageous and leads to high yields in functional LV. However, for a further improvement and cost-reduction of the LV production process, optimization of the critical process parameter harvest rate will be required. The characteristic process phases identified here will be useful for an advanced process supervision. For example, the harvest rate could be controlled as a function of the expected LV titer in each production phase. This strategy could be used to minimize medium consumption and provide constant functional particle concentrations in the harvest for optimized downstream processing.

3.1.2. Comparison of off- and online methods for monitoring of LV production

Similar LV production kinetics and monitoring results were observed in several bioreactor perfusion cultures under different operating conditions (Fig. 2) and can be described using the same phase distribution pattern. Whereas the transition phases 1–3 were easily distinguished, it was generally more difficult to identify the beginning of culture phase 4. During process phase 1 (0–24 hpt) and the transition into phase 2 (24–50/70 hpt), a single maximum value for the oxygen sparging rate (OSR) was observed, coinciding with the maximum biovolume and permittivity. In contrast, the total GFP expression attained high levels only in phases 3 and 4, with the culture at 1 VVD resulting in higher values than the cultivations at 2 VVD.

In all of the cultures, the cell diameter was found to initially decrease after the transfection, but eventually increased at the transition into phase 2. During the second phase, decreases in cell size, $\Delta\varepsilon_{\max}$, $\Delta\varepsilon_{f_c}/\Delta\varepsilon_{0.6}$ MHz and OSR were also observed, while viability remained high in all cases. The diameter returned to its initial value that was observed before transfection during phase 2 and increased significantly thereafter (until phase 4).

The maximum in OSR might also be used as an indicator of the initial LV release and the onset of the production phase. Changes in oxygen consumption during viral production are well documented in the literature [46–48]. During LV production, however, monitoring of OSR alone seemed to provide considerably less direct information specific to the titer kinetics than $\Delta\varepsilon_{\max}$ and *fc*.

If GFP is the transgene encoded by the viral vector construct, the monitoring of GFP expression can also provide an indication of the infection and production kinetics of viral vectors [33,49]. This also holds for the production of VSV-G pseudotyped LVs in which self-infection of the producer cells results in high transgene expression once LVs are released [50,51]. In small-scale experiments, the peak production after 48 hpt and the GFP expression measured at 72 and 96 hpt correlated well over a wide titer range (results not shown). In bioreactor-scale cultivations, a lower perfusion rate resulted in less GFP expression in the producer cells, possibly due to an increased residence time of functional particles in the vessel. The use of *in situ* GFP probes might therefore be explored during LV production [52]. However, the value of these measurements will be most likely limited because information on the functional viral titer would only be available after a delay of 1 or 2 days. More importantly, once GFP will be replaced by a different transgene of interest, this method will be inapplicable.

3.1.3. Changes in online permittivity signals as indicator of LV yield

During BEV production and after synchronous infection of the producer cells, a plateau region can be monitored less than 20 h post-infection. This temporary leveling of the permittivity signal corresponds to the first viral release and the onset of BEV production [18,19,53]. Similar to BEVs, LVs bud off from the producer cell membrane. It was thus investigated to determine whether the permittivity signal variations were related to this budding process and, as a consequence, are a function of the LV yield. During LV production, the ratio of functional to total particles is generally low with the expression of LV proteins such as Gag and VSV-G being sufficient for the release of non-functional enveloped particles [45,54–60]. All of these species share similar properties in that they bud off from the membrane and hence directly impact its structure and properties. They were also found to contain viral or cellular DNA/RNA [58,59] which leads to an overestimation of VG titer.

Knowing that permittivity is a function of the cellular membrane properties, we therefore evaluated if the relative changes in the two key β-dispersion parameters (*fc* and $\Delta\varepsilon_{\max}$) during the viral release phase (phase 2) could give indications on the total LV yield from the bioreactor runs. We found a good correlation of the relative changes in *fc* and $\Delta\varepsilon_{\max}$, calculated as the difference of each of these values at the end of phase 1 and phase 2, and the total VG yield from bioreactor LV productions (Fig. 3). This means that the amount of total viral particles released during the cultures was reflected in the online signals acquired during the viral release phase. However, as the range in the viral yield with 3×10^{12}–8×10^{13} vg/run was rather limited, these results will need to be confirmed by future cultures. In contrast, the total GTA titer yield did not correlate with the signal variations (data not shown). It was observed that both the permittivity signal and the production of functional particles continuously decreased starting in phase 2. It is believed that the loss of the VSV-G expression due to its cytotoxic effects [58–61] and/or the lysis of producer cells induced by its cytotoxicity caused the differences in VG and GTA titer during phases 3 and 4 (Section 3.1.1, Figs. 1 and 2).

Permittivity measurements thus provide an indication on process yields and it can be expected that the online signal will allow assessing the success of transfection or process failure. If the correlation of productivity and signal changes can be confirmed over a wider range of production yields, permittivity monitoring would represent a real-time tool to assess process yields in LV production processes. Such tools, providing viral release and titer detection in real-time and without sampling, would dramatically facilitate process development, i.e., in the optimization of production conditions, improvement of process robustness and reduction in yield variation.

3.2. Analysis of permittivity signals

3.2.1. Comparison of biovolume and permittivity measurements

We sought to further analyze the evolution of the online permittivity signals by comparing our data with offline biovolume (*bv*) measurements. The *bv* can be used as an offline estimate of the online permittivity value, particularly during the exponential growth phase and when viability remains high [19,53]. More specifically, the dual-frequency permittivity ($\Delta\varepsilon_{f_c}/\Delta\varepsilon_{0.6}$ MHz) or, if using $bv * d/2$, the permittivity increment ($\Delta\varepsilon_{\max}$), generally correlates well with the biovolume evolution [see Eq. (2)]; in preliminary batch cultures of the HEK293 producer cells, we could, for example, observe a linear relationship of $\Delta\varepsilon_{\max}$ and $bv * d/2$ throughout the entire culture (data for batch culture not completely shown). In general, during the exponential growth phase of batch cultures and before transfection during LV production runs, a good correla-

Please cite this article in press as: S. Ansorge, et al., Monitoring lentiviral vector production kinetics using online permittivity measurements, Biochem. Eng. J. (2011), doi:10.1016/j.bej.2011.01.002

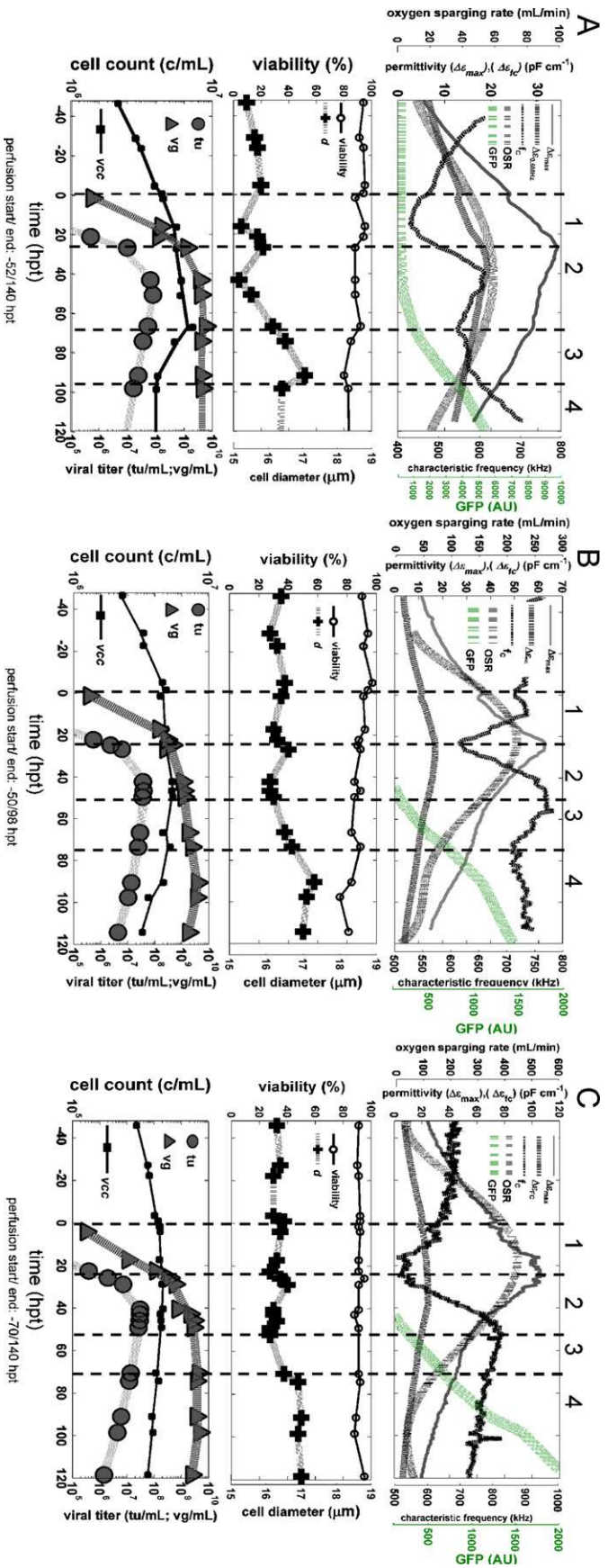

Fig. 2. Monitoring results for high-yield LV production runs. Three independent experiments are shown for comparison. The culture in (B) is identical to the one presented in Figs. 3 and 5. Operating conditions varied with: (A) perfusion rate in volume(s) of medium per reactor volume and day (VVD), *vcc* at time of transfection: 1 VVD, 4.4×10^6 *vcc*; (B) 2 VVD, 4.7×10^6 *vcc*; (C) 2 VVD, 8×10^6 *vcc*; for cultivations shown in A and B, the same medium composition (HyQ) was used; culture shown in C included additional supplementation with CB5 (HyQ+).

Please cite this article in press as: S. Ansorge, et al., Monitoring lentiviral vector production kinetics using online permittivity measurements, Biochem. Eng. J. (2011), doi:10.1016/j.bej.2011.01.002

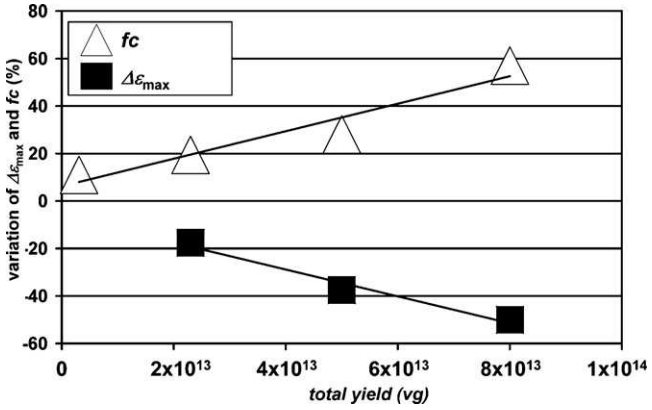

Fig. 3. Relative changes in permittivity-related parameters ($\Delta\varepsilon_{max}$ and f_C) indicate total process yield; $\Delta\varepsilon_{max}$: $R^2 = 0.97$; f_C: $R^2 = 0.93$. The changes were calculated by taking the values of $\Delta\varepsilon_{max}$ and f_C at the end of phases 1 and 2, respectively. Similar high regression coefficients were found when plotting the total yield after 2 dpt (not shown); one value for $\Delta\varepsilon_{max}$ for a culture at low yield in which the maximum was related to a cease in cell growth was omitted in the graph.

tion ($R^2 = 0.93$) was observed between $bv * d/2$ and the permittivity increment $\Delta\varepsilon_{max}$ (Fig. 4A). However, the samples taken after transfection, i.e., during process phases 1 and 2, did not follow the same trend. These samples are represented in Fig. 4A as squares; samples taken during phase 1 and at the transition from phases 1 and 2, i.e., at the maximum of $\Delta\varepsilon_{max}$ and the minimum in *fc*, are highlighted by a dotted circle. In contrast, the samples from process phases 3–4 were again in line with the correlation with the exception of those corresponding to the last day of the cultivation (90–114 hpt; marked by a dashed circle).

The characteristic frequency (*fc*) is directly affected by changes in cell diameter, intracellular conductivity and membrane capacitance [Eq. (3)]. The *fc* was consequently plotted against the inverse of the offline measured cell radius $1/(d/2)$ (Fig. 4B). Although a linear relationship between the two variables was apparent, the regression coefficient was rather low ($R^2 = 0.6$), even when the values obtained from process phases 1 and 2 at and around the maximum in $\Delta\varepsilon_{max}$, the minimum in *fc* (dotted circle) and the late stages of the culture (dashed circle) were excluded from the regression.

The cell diameter (d) reached a first maximum at the beginning of the viral release phase (Fig. 2), which was in line with the maximum in $\Delta\varepsilon_{max}$ and the minimum in *fc*; it is thus evident that the changes in cell diameter played a role in the evolution of $\Delta\varepsilon_{max}$ and *fc*. However, this cell diameter increase was not sufficient to explain the dramatic increase in $\Delta\varepsilon_{max}$ and the decrease in *fc* from ~10 to 20 hpt.

Values for samples from the very end of the cultivation generally deviated from the correlations; the remaining cells showed a lower permittivity per biovolume and a higher *fc* per $1/(d/2)$. A considerable amount of cell debris was observed during phase 4, accompanied by an attachment of biomass to the inner surface of the bioreactor/shake flask, and cell aggregation was increased. It is therefore possible that the dielectric properties of the culture were altered towards the end of the cultivation. This would be in line with the observations by others which found that the permittivity measurements cease to predict the biovolume in late cultivation phases [62,63], particularly when viability decreases and membrane conductance rises, which results in a lower cell-specific permittivity [42].

The results from Fig. 4A and B thus indicate that neither cell density nor cell diameter were solely responsible for the observed changes in the permittivity increment and the characteristic frequency after transfection. During phases 1 and 2, i.e., before and

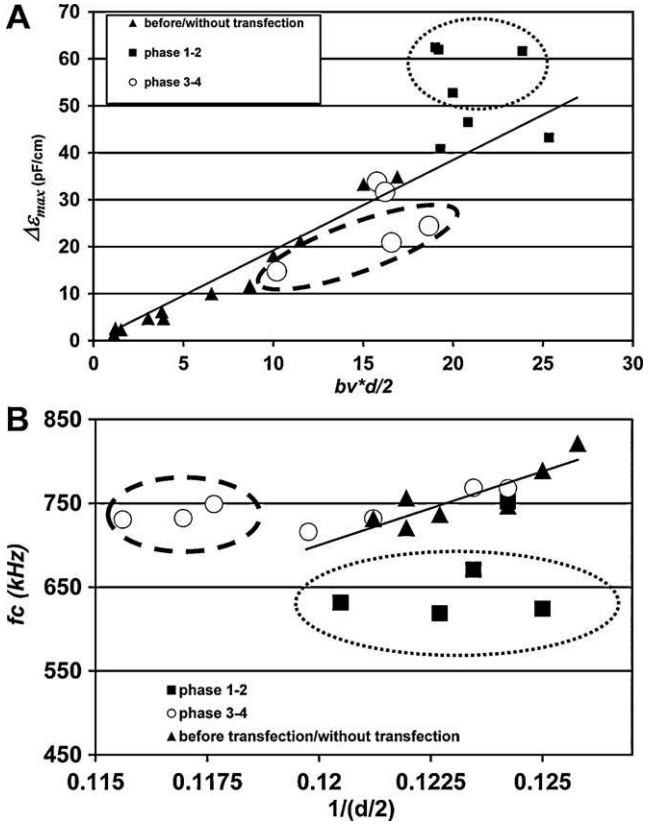

Fig. 4. Regression lines for $\Delta\varepsilon_{max}$ and $bv * d/2$ (A) and f_C and the inverse of the mean cell radius $d/2$ (B); this plot was drawn assuming a constant value of C_M (see Eqs. (1)–(3) for the theoretical relationship of the variables). *bv* was calculated for each sample using the mean cell diameter (d) and the cell density (N) [Eq. (1)]. Regressions were in both figures calculated based only on samples from the exponential growth phase in batch and before transfection in perfusion (triangles); regression coefficients were: $R^2 = 0.93$ (A) and $R^2 = 0.6$ (B). Dashed circles mark samples at the end of the culture for which viability was low; dotted circles mark samples after transfection in process phase 1/the beginning of phase 2, i.e., at and around the maximum in $\Delta\varepsilon_{max}$ and the minimum in f_C. The values from the perfusion culture correspond to the cultivation shown in Figs. 1, 2B and 5. Similar correlations between $bv * d/2$ and $\Delta\varepsilon_{max}$, and between cell diameter and *fc* were found for all other experiments in which LV were produced at high yield. In contrast, for non-producing batch cultures, we did not observe these deviations at the maximum value of $\Delta\varepsilon_{max}$ (regressions not shown for all cultures).

at the time of viral release, $\Delta\varepsilon_{max}$ increased and *fc* decreased to a larger extent than was expected from the changes in *vcc* and *d*.

3.2.2. Multifrequency permittivity spectra

To further investigate the changes in β-dispersion parameters, the permittivity spectra were analyzed after mean centering and variance scaling (Fig. 5). Attributing the same weight to the permittivity signals at the different frequencies allows the dielectric parameter which most likely causes the observed changes in the spectrum to be inferred.

Before transfection, the permittivity showed the same response at all frequencies within the β-dispersion range. After transfection, changes in the permittivity spectra occurred at 8–12 hpt when a first inflection point (indicated by an arrow) in the data became apparent. At that time, the permittivity measured at low frequencies (0.3–1 MHz) increased at a much faster rate than the permittivity measured at high frequencies (2–10 MHz). A second inflection point was then observed at ~32 to 40 hpt (indicated by an arrow), after which the permittivity at lower frequencies decreased more rapidly than at high frequencies. This second inflection point in the permittivity spectrum coincided with the minimum in cell diameter. The inflection points were thus observed

Please cite this article in press as: S. Ansorge, et al., Monitoring lentiviral vector production kinetics using online permittivity measurements, Biochem. Eng. J. (2011), doi:10.1016/j.bej.2011.01.002

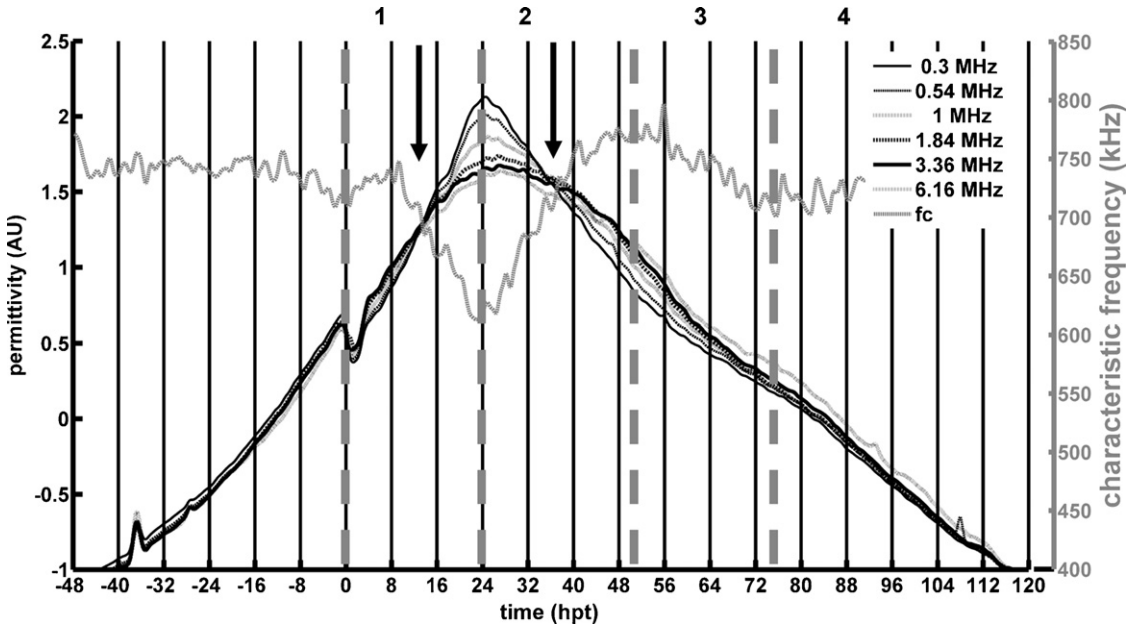

Fig. 5. Inflection points (marked by arrows) in the mean-centered and variance-scaled permittivity spectrum indicate changes in the dielectric properties of producer cells after transfection; grey dashed lines mark process transition phases 1–4. See text for details.

before the minimum in *fc* and after the maximum in $\Delta\varepsilon_{max}$, respectively.

If no significant changes in cell diameter, intracellular conductivity and membrane capacitance occur, the response at all frequencies should be identical [Eqs. (2) and (3)]. This is the situation observed prior to transfection, wherein only the amplitude of the β-dispersion ($\Delta\varepsilon_{max}$), but not its shape (*fc*), changed. After transfection, it is likely that an increase in C_M occurred starting at ~8 to 12 hpt. At that time, the impact of these changes was monitored in the permittivity spectrum. Following the permittivity theory, [Eqs. (1)–(3)], these changes must have been due to an increase of either C_M or *d*. Changes in *d* were ruled out earlier (Fig. 4), and a variation in σ_i alone during phases 1 and 2 can be equally excluded based on these data. Yet, it is still possible that σ_i changed in parallel to the variations in cell diameter and C_M.

As a result, it is believed that the permittivity variations were essentially related to an increase in C_M before and at the time of viral release. At that time, the maximum in $\Delta\varepsilon_{max}$ and the minimum in *fc* were observed, and we attributed these changes to the LV budding process, which directly affects the cellular membrane properties.

C_M was originally reported to be a biological constant with values in the range of $1 \pm 0.5\ \mu F/cm^2$ and described as a measure of the 'wrinkliness' of the cell membrane [37,40,42]. More recent studies found, however, that C_M changes after the viral infection and overexpression of cation channels [23,64]. Therefore, it seems to be particularly affected by processes involving the cellular membrane properties, such as exocytosis (loss of microvilli), viral release, and apoptosis [42,65]. Reductions in C_M of 40–60% were reported for several cell types after infection with different viruses, such as the herpes simplex virus and polyomavirus. C_M is affected as early as a few hours post-infection as a result of the loss of membrane blebs and a more uniform membrane conformation or a membrane surface with more irregularities [22,23].

These findings thus support our observations made for LV. In addition, for HIV-1, from which LV are derived, it is hypothesized that the release of virus by membrane budding and fission takes place very shortly after the formation of particles [66]. It is also known that the production of HIV-forming proteins is initiated as early as 5–6 h after transfection [67]. These processes, and in turn the changes in dielectric properties of the producer cells, would be consistent with the early changes observable in the permittivity spectra at the first inflection point (Fig. 5). Thus, based on the results presented in Fig. 4A and B, the initial LV release causes a temporary increase in the value of C_M of 30–70%.

4. Conclusion

To our knowledge, this is the first study presenting multifrequency permittivity measurements as online monitoring tools for the detection of viral release after transfection. Previously reported observations were made for systems in which viral vectors are produced after the infection of producer cells. These studies mainly focused on the monitoring of the increase in biovolume of insect cells during BEV production and did not further analyze permittivity spectra or β-dispersion parameters (dielectric increment $\Delta\varepsilon_{max}$ and characteristic frequency *fc*). In the present work, four distinct and reproducible process transition phases were identified during LV production based on the online permittivity data. These phases were shown to be related to the initial release of LVs and the kinetics of functional viral particle titers. Extrema and slope changes in the β-dispersion parameters ($\Delta\varepsilon_{max}$, *fc*) indicated first viral release (~24 hpt), the maximum functional viral (~48 hpt) and the time at which LV productivity had decreased significantly (>72–96 hpt). The relative changes in $\Delta\varepsilon_{max}$ and *fc* correlated with the yield in total viral particles (VG titer) of several independent cultivations. The permittivity variations during LV production were further analyzed in this work. During the viral release phase, the culture exhibited higher permittivity values per biovolume and a decreased characteristic frequency (*fc*) per cell diameter. The changes in cell size and cell density were not sufficient to explain the differences in $\Delta\varepsilon_{max}$, $\Delta\varepsilon_{fc}$ and *fc*. We conclude that permittivity measurements detect the physiological changes in producer cells caused by the LV budding process; viral production and release were consequently responsible for the characteristic profile of the real-time permittivity signals.

Please cite this article in press as: S. Ansorge, et al., Monitoring lentiviral vector production kinetics using online permittivity measurements, Biochem. Eng. J. (2011), doi:10.1016/j.bej.2011.01.002

It was inferred that membrane capacitance (C_M) must have increased significantly after transfection and around the time of first viral release. However, the changes of cell membrane properties (C_M) during LV production were not directly measured. It is consequently possible that either the other dielectric parameters (such as the intracellular conductivity) were affected or that changes in the producer cell population due to the cytotoxic effects of the LV proteins contributed to the permittivity variations. The use of methods such as dielectrophoresis and electrorotation in combination with suitable control cultures and/or alternative LV envelopes should be of interest in this context. Such experiments should shed light on the events occurring at the cellular level and to a better understanding of the interrelation between LV release and the dielectric properties of cells. Yet, it is not necessary to unambiguously identify the dielectric parameter(s) affected during LV production to use the observations presented here for process characterization, development, optimization and control. Compared to other methods (oxygen consumption, total GFP expression), dielectric spectroscopy appeared to be the most sensitive and informative tool for online monitoring of LV production as it appeared to be sensitive to changes at the cellular membrane level. The use of changes in $\Delta\varepsilon_{max}$, $\Delta\varepsilon_{f_c}$ and fc as a PAT tool, as guiding variables for the real-time identification of action points or for the direct control of critical process parameters such as perfusion rate and final harvest time is highly recommended and should allow optimizing LV production processes. Our findings will not only facilitate LV production process characterization and modelization but also enable advanced process control to further support the establishment of robust lentiviral vector production in large-scale and to reduce process variability through accelerated process development. Additionally, it is expected that the findings reported herein could be translated to other viral vector and vaccine production processes based on transient transfection and infection.

Acknowledgements

The authors would like to acknowledge Bernard Massie for graciously providing the lentiviral vector plasmids. The essential support of G. St-Laurent (plasmid production, PCR method), L. Bourget (flow cytometry analysis), Y. Durocher, S. Perret, L. Bisson, B. Cass (cell maintenance, cell culture techniques and transfection protocols and support), R. Voyer and R. Ochoa (bioreactor setup) is greatly appreciated. A beta-version of the Biomass 400 system was graciously provided by Fogale nanotech. Permittivity spectra were pretreated and analyzed thanks to the essential support from G. Esteban (Fogale nanotech). The help of Daniel Logan and Matthew Lee (Aber Instruments) during the analysis with the AberScan software as well as E. Petiot for a critical review of this manuscript was also highly appreciated.

References

[1] A.S. Cockrell, T. Kafri, Gene delivery by lentivirus vectors, Mol. Biotechnol. 36 (3) (2007) 184–204.
[2] K. Pluta, W. Diehl, X.Y. Zhang, R. Kutner, A. Bialkowska, J. Reiser, Lentiviral vectors encoding tetracycline-dependent repressors and transactivators for reversible knockdown of gene expression: a comparative study, BMC Biotechnol. 7 (2007) 41.
[3] E. Vigna, L. Naldini, Lentiviral vectors: excellent tools for experimental gene transfer and promising candidates for gene therapy, J. Gene Med. 2 (5) (2000) 308–316.
[4] S. Ansorge, O. Henry, A. Kamen, Recent progress in lentiviral vector mass production, Biochem. Eng. J. 48 (3) (2010) 362–377.
[5] O.W. Merten, State-of-the-art of the production of retroviral vectors, J. Gene Med. 6 (S1) (2004) S105–S124.
[6] R.E. Throm, A.A. Ouma, S. Zhou, A. Chandrasekaran, T. Lockey, M. Greene, S.S. De Ravin, M. Moayeri, H.L. Malech, B.P. Sorrentino, J.T. Gray, Efficient construction of producer cell lines for a SIN lentiviral vector for SCID-X1 gene therapy by concatemeric array transfection, Blood 113 (21) (2009) 5104–5110.
[7] J.F. Wright, Transient transfection methods for clinical adeno-associated viral vector production, Hum. Gene Ther. 20 (2009) 1–9.
[8] J.Y. Park, B.P. Lim, K. Lee, Y.G. Kim, E.C. Jo, Scalable production of adeno-associated virus type 2 vectors via suspension transfection, Biotechnol. Bioeng. 94 (3) (2006) 416–430.
[9] L. Baldi, D. Hacker, M. Adam, F. Wurm, Recombinant protein production by large-scale transient gene expression in mammalian cells: state of the art and future perspectives, Biotechnol. Lett. 29 (5) (2007) 677–684.
[10] Y. Durocher, P.L. Pham, G. St-Laurent, D. Jacob, B. Cass, P. Chahal, C.J. Lau, J. Nalbantoglu, A. Kamen, Scalable serum-free production of recombinant adeno-associated virus type 2 by transfection of 293 suspension cells, J. Virol. Methods 144 (1–2) (2007) 32–40.
[11] M. Hildinger, L. Baldi, M. Stettler, F. Wurm, High-titer, serum-free production of adeno-associated virus vectors by polyethyleneimine-mediated plasmid transfection in mammalian suspension cells, Biotechnol. Lett. (2007).
[12] S. Geisse, Reflections on more than 10 years of TGE approaches, Protein Expr. Purif. 64 (2) (2009) 99–107.
[13] B.H. Junker, H.Y. Wang, Bioprocess monitoring and computer control: key roots of the current PAT initiative, Biotechnol. Bioeng. 95 (2) (2006) 226–261.
[14] A.P. Teixeira, R. Olivera, P.M. Alves, M.J.T. Carrondo, Advances in on-line monitoring and control of mammalian cell cultures: supporting the PAT initiative, Biotechnol. Adv. 27 (6) (2009) 726–732.
[15] B. Sonnleitner, G. Locher, A. Fiechter, Biomass determination, J. Biotechnol. 25 (1–2) (1992) 5–22.
[16] L. Olsson, J. Nielsen, On-line and in situ monitoring of biomass in submerged cultivations, Trends Biotechnol. (15) (1997) 517–522.
[17] K. Kiviharju, K. Salonen, U. Moilanen, E. Meskanen, M. Leisola, T. Eerikäinen, On-line biomass measurements in bioreactor cultivations: comparison study of two on-line probes, J. Ind. Microbiol. Biotechnol. 34 (8) (2007) 561–566.
[18] A. Zeiser, C. Bedard, R. Voyer, B. Jardin, R. Tom, A.A. Kamen, On-line monitoring of the progress of infection in Sf-9 insect cell cultures using relative permittivity measurements, Biotechnol. Bioeng. 63 (1) (1999) 122–126.
[19] A. Zeiser, C.B. Elias, R. Voyer, B. Jardin, A.A. Kamen, On-line monitoring of physiological parameters of insect cell cultures during the growth and infection process, Biotechnol. Prog. 16 (5) (2000) 803–808.
[20] C. Cannizzaro, R. Gugerli, I. Marison, U. von Stockar, On-line biomass monitoring of CHO perfusion culture with scanning dielectric spectroscopy, Biotechnol. Bioeng. 84 (5) (2003) 597–610.
[21] S. Ansorge, G. Esteban, G. Schmid, Multifrequency permittivity measurements enable on-line monitoring of changes in intracellular conductivity due to nutrient limitations during batch cultivations of CHO cells, Biotechnol. Prog. 26 (1) (2010) 272–283.
[22] S. Archer, H. Morgan, F.J. Rixon, Electrorotation studies of baby hamster kidney fibroblasts infected with herpes simplex virus type 1, Biophys. J. 76 (5) (1999) 2833.
[23] V. Berardi, C. Aiello, A. Bonincontro, G. Risuleo, Alterations of the plasma membrane caused by murine polyomavirus proliferation: an electrorotation study, J. Membr. Biol. 229 (1) (2009) 19–25.
[24] E. Chico, V. Jäger, Measurements of changes in cell size distribution to monitor Baculovirus infection of insect cells, in: O.W. Merten, P. Perrin, B. Griffiths (Eds.), New Developments and New Applications in Animal Cell Technology, Kluwer Academic Publishers, Dordrecht, 1998, pp. 329–331.
[25] L. Palomares, J. Pedroza, O. Ramirez, Cell size as a tool to predict the production of recombinant protein by the insect-cell baculovirus expression system, Biotechnol. Lett. 23 (5) (2001) 359.
[26] A. Negrete, G. Esteban, R.M. Kotin, Process optimization of large-scale production of recombinant adeno-associated vectors using dielectric spectroscopy, Appl. Microbiol. Biotechnol. 76 (4) (2007) 761–772.
[27] S. Cecchini, A. Negrete, R.M. Kotin, Toward exascale production of recombinant adeno-associated virus for gene transfer applications, Gene Ther. 15 (11) (2008) 823–830.
[28] J. Côté, A. Garnier, B. Massie, A. Kamen, Serum-free production of recombinant proteins and adenoviral vector by 293-SF-3F6 cells, Biotechnol. Bioeng. 59 (1998) 567–575.
[29] S. Ansorge, S. Lanthier, J. Transfiguracion, Y. Durocher, O. Henry, A. Kamen, Development of a scalable process for high-yield lentiviral vector production by transient transfection of HEK293 suspension cultures, J. Gene Med. 11 (10) (2009) 868–876.
[30] T. Dull, R. Zufferey, M. Kelly, R.J. Mandel, M. Nguyen, D. Trono, L. Naldini, A third-generation lentivirus vector with a conditional packaging system, J. Virol. 72 (11) (1998) 8463–8471.
[31] S. Broussau, N. Jabbour, A. Mullick, Y. Durocher, R. Tom, J. Transfiguracion, R. Gilbert, B. Massie, Inducible packaging cells for large-scale production of lentiviral vectors in serum-free suspension culture, Mol. Ther. 16 (3) (2008) 500–507.
[32] M.M. Segura, A. Garnier, Y. Durocher, H. Coelho, A. Kamen, Production of lentiviral vectors by large-scale transient transfection of suspension cultures and affinity chromatography purification, Biotechnol. Bioeng. 98 (4) (2007) 789–799.
[33] O. Henry, E. Dormond, M. Perrier, A. Kamen, Insights into adenoviral vector production kinetics in acoustic filter-based perfusion cultures, Biotechnol. Bioeng. 86 (7) (2004) 765–774.
[34] A. Garnier, R. Voyer, R. Tom, S. Perret, B. Jardin, A. Kamen, Dissolved carbon dioxide accumulation in a large scale and high density production of TGFβ receptor with baculovirus infected Sf-9 cells, Cytotechnology 22 (1996) 53–63.

Please cite this article in press as: S. Ansorge, et al., Monitoring lentiviral vector production kinetics using online permittivity measurements, Biochem. Eng. J. (2011), doi:10.1016/j.bej.2011.01.002

[35] P. Winkelmeier, B. Glauner, T. Lindl, Quantification of cytotoxicity by cell volume and cell proliferation, ATLA 21 (1993) 269–280.
[36] K. Frame, W.-S. Hu, Cell volume measurement as an estimation of mammalian cell biomass, Biotechnol. Bioeng. 36 (1990) 191–197.
[37] D.B. Kell, C.M. Harris, Dielectric spectroscopy and membrane organization, J. Bioelectricity 4 (1985) 317–348.
[38] C.M. Harris, R.W. Todd, S.J. Bungard, J.G.M. Lovitt, D.B. Kell, Dielectric permittivity of microbial suspensions at radio frequencies: a novel method for the real-time estimation of microbial biomass, Enzyme Microb. Technol. 9 (1987) 181–186.
[39] R. Pethig, D.B. Kell, The passive electrical properties of biological systems: their significance in physiology, biophysics and biotechnology, Phys. Med. Biol. 32 (1987) 933–970.
[40] G.H. Markx, C.L. Davey, The dielectric properties of biological cells at radiofrequencies: applications in biotechnology, Enzyme Microb. Technol. 25 (1999) 161–171.
[41] H.P. Schwan, Electrical properties of tissue and cell suspensions, Adv. Biol. Med. Phys. 5 (1957) 147–208.
[42] P.M. Patel, G.H. Markx, Dielectric measurement of cell death, Enzyme Microb. Technol. 43 (7) (2008) 463–470.
[43] K.S. Cole, R.H. Cole, Dispersion and absorption in dielectrics: 1 – alternating current characteristics, J. Chem. Phys. 9 (1929) 341–351.
[44] C.L. Davey, The Biomass Monitor Source Book, Aberystwyth, Department of Biological Sciences, University of Wales, 1993.
[45] F. Higashikawa, L.-J. Chang, Kinetic analyses of stability of simple and complex retroviral vectors, Virology 280 (1) (2001) 124–131.
[46] C.M. Kussow, et al., Monitoring of mammalian cell growth and virus production process using on-line oxygen uptake rate measurement, Enzyme Microb. Technol. 17 (9) (1995) 779.
[47] A.A. Kamen, C. Bédard, R. Tom, S. Perret, B. Jardin, On-line monitoring of respiration in recombinant-baculovirus infected and uninfected insect cell bioreactor cultures, Biotechnol. Bioeng. (50) (1996) 36–48.
[48] M. Lecina, A. Soley, J. Gràcia, E. Espunya, B. Lázaro, J.J. Cairó, F. Gòdia, Application of on-line OUR measurements to detect actions points to improve baculovirus-insect cell cultures in bioreactors, J. Biotechnol. 125 (3) (2006) 385–394.
[49] A. Kamen, O. Henry, Development and optimization of an adenovirus production process, J. Gene Med. 6 (S1) (2004) S184–S192.
[50] D. Farson, R. Witt, R. McGuinness, T. Dull, M. Kelly, J. Song, R. Radeke, A. Bukovsky, A. Consiglio, L. Naldini, A new-generation stable inducible packaging cell line for lentiviral vectors, Hum. Gene Ther. 12 (8) (2001) 981–997.
[51] C. Bagnis, P. Bailly, S. Chapel-Fernandes, Using an EGFPmeter to evaluate the lentiviral vector production: tricks and traps, in: Viral Applications of Green Fluorescent Protein, 2009, pp. 151–163.
[52] P.-A. Gilbert, A. Garnier, D. Jacob, A. Kamen, On-line measurement of green fluorescent protein (GFP) fluorescence for the monitoring of recombinant adenovirus production, Biotechnol. Lett. 22 (7) (2000) 561–567.
[53] S. Ansorge, G. Esteban, G. Schmid, On-line monitoring of infected Sf-9 insect cell cultures by scanning permittivity measurements and comparison with off-line biovolume measurements, Cytotechnology 55 (2007) 115–124.
[54] K. Haglund, J. Forman, H.-G. Kräusslich, J.K. Rose, Expression of human immunodeficiency virus type 1 Gag protein precursor and envelope proteins from a vesicular stomatitis virus recombinant: high-level production of virus-like particles containing HIV envelope, Virology 268 (1) (2000) 112–121.
[55] H. Göttlinger, The HIV-1 assembly machine, AIDS 15 (Suppl. 5) (2001) S13–20.
[56] N.M. Sherer, M.J. Lehmann, L.F. Jimenez-Soto, A. Ingmundson, S.M. Horner, G. Cicchetti, P.G. Allen, M. Pypaert, J.M. Cunningham, W. Mothes, Visualization of retroviral replication in living cells reveals budding into multivesicular bodies, Traffic 4 (11) (2003) 785–801.
[57] B. Mitta, M. Rimann, M. Fussenegger, Detailed design and comparative analysis of protocols for optimized production of high-performance HIV-1-derived lentiviral particles, Metab. Eng. 7 (5–6) (2005) 426–436.
[58] A. Pichlmair, S.S. Diebold, S. Gschmeissner, Y. Takeuchi, Y. Ikeda, M.K. Collins, C. Reis e Sousa, Tubulovesicular structures within vesicular stomatitis virus G protein-pseudotyped lentiviral vector preparations carry DNA and stimulate antiviral responses via Toll-like receptor 9, J. Virol. 81 (2007) 539–547.
[59] Y. Zhao, K. Keating, C. Dolman, R. Thorpe, Characterization of complete particles (VSV-G/SIN-GFP) and empty particles (VSV-G/EMPTY) in human immunodeficiency virus type 1-based lentiviral products for gene therapy: potential applications for improvement of product quality and safety, Hum. Gene Ther. 19 (5) (2008) 475–486.
[60] Y. Li, C. Drone, E. Sat, H.P. Ghosh, Mutational analysis of the vesicular stomatitis virus glycoprotein G for membrane fusion domains, J. Virol. 67 (7) (1993) 4070–4077.
[61] R. Quinonez, R.E. Sutton, Lentiviral vectors for gene delivery into cells, DNA Cell Biol. 21 (12) (2002) 937–951.
[62] P. Ducommun, I. Bolzonella, M. Rhiel, P. Pugeaud, U. von Stockar, I.W. Marison, On-line determination of animal cell concentration, Biotechnol. Bioeng. 72 (5) (2001) 515–522.
[63] P. Ducommun, A. Kadouri, U. von Stockar, I.W. Marison, On-line determination of animal cell concentration in two industrial high-density culture processes by dielectric spectroscopy, Biotechnol. Bioeng. 77 (3) (2002) 316–323.
[64] D. Zimmermann, A. Zhou, M. Kiesel, K. Feldbauer, U. Terpitz, W. Haase, T. Schneider-Hohendorf, E. Bamberg, V.L. Sukhorukov, Effects on capacitance by overexpression of membrane proteins, Biochem. Biophys. Res. Commun. 369 (4) (2008) 1022–1026.
[65] P.M. Patel, A. Bhat, G.H. Markx, A comparative study of cell death using electrical capacitance measurements and dielectrophoresis, Enzyme Microb. Technol. 43 (7) (2008) 523–530.
[66] T. Goto, K. Ikuta, J.J. Zhang, C. Morita, K. Sano, M. Komatsu, H. Fujita, S. Kato, M. Nakai, The budding of defective human immunodeficiency virus type 1 (HIV-1) particles from cell clones persistently infected with HIV-1, Arch. Virol. 111 (1) (1990) 87–101.
[67] N. Jouvenet, P.D. Bieniasz, S.M. Simon, Imaging the biogenesis of individual HIV-1 virions in live cells, Nature 454 (7201) (2008) 236–240.

Please cite this article in press as: S. Ansorge, et al., Monitoring lentiviral vector production kinetics using online permittivity measurements, Biochem. Eng. J. (2011), doi:10.1016/j.bej.2011.01.002